The Seybold Report

ISSN 1533-9211

DOI 10.5281/zenodo.7220825

INVESTIGATION OF BZT BASED PVDF POLYMER MATERIALS: MICROCRYSTALLINE, MORPHOLOGICAL AND ITS ELECTRICAL BEHAVIOUR STUDY

RAKESH M[1], NARENDRA BABU B. R[2], PREMA N. S[3], VIJAY KASHIMATT M. G[4] and UDAYASHANKAR S[5]

[1]Department of Biomedical & Robotic Engineering, Mysore University School of Engineering, University of Mysore, Mysuru, India. Email: raki.hombale@gmail.com
[2]Department of Mechanical Engineering, Vidya Vikas Institute of Engineering & Technology, Mysure, India. Email: narenbabu8@gmail.com
[3]Department of Information Science and Engineering, Vidyavardhaka College of Engineering, Mysuru, India. Email: prema.gowda@gmail.com
[4]Department of Mechanical Engineering, Siddaganga Institute of Technology, Tumkur, India. Email: vijaykashimatt.mg@gmail.com
[5]Department of Mechanical Engineering, BTLITM, Bengaluru, Karnataka, India. Email: udaya_creative@yahoo.com

Abstract:

Since from many decades man is being using natural resources in many ways in this society, he has also conserved energy, which has made him too led comfort life. Advancement of conductive polymers heavily relies on the study of various piezoelectric rich polymer energy sources and their features since these materials are the easiest to come by in nature, affordable, environmentally acceptable, and have strong electrical potency. In the present research work Barium Zirconate Titanate (BZT) is a piezoelectric enhanced material and its performance is studied. By using the hydrothermal approach and the Co-precipitate gel technique, BZT nano materials were effectively synthesized and studied the electrical behavior performances. The BZT nano composite synthesized, exhibited Ba ($Zr_{0.25}Ti_{0.75}$) O_3) phase was added polyvinylidene fluoride (PVDF) polymer matrix which was prepared by simple solvent casting process. The XRD and SEM have revealed purity phase and formation of BZT nano particles have composited along with α and β-phase PVDF polymer. The prime electrical properties such as dielectric conductivity, dielectric loss, and dielectric constant parameters of Barium Zirconate Titanate (BZT)-polyvinylidene fluoride (PVDF) were evaluated and further analyzed in detail with consideration of different frequencies in dielectric studies. Maximum dielectric loss with regard to frequency was observed in 0.5%BZT-PVDF films, which have witnessed for high dielectric stability, and the conductivity was raised with 0.5%BZT based PVDF polymer films as compared to pure PVDF polymer. Our experimental studies demonstrate the strong frequency dependence of dielectric parameters including real and imaginary modulus as well as dielectric loss. Additionally, the investigation has provided convincing evidence for the pure PVDF polymer film's melting point and dynamic mechanical analysis (DMA), which helps us understand the stability of conductive polymers.

Keywords: BZT, Dielectric, PVDF, XRD, SEM, DMA, Polymer, Nanocomposites, Hydrothermal.

1. INTRODUCTION

The fabrication of ceramic composites and its technology is well developed and has been explained in many books, review papers, and research articles dedicated to various aspects of PZT, BZT processing. There are various techniques employed to synthesis ceramic materials such as Sol gel process, solid state method, gel-precipitate method, hydrothermal autoclave etc.

The Seybold Report
ISSN 1533-9211
DOI 10.5281/zenodo.7220825

Due to their exceptional productivity, economic factor, and ease of processing, perovskite-based nanomaterials have been regarded as favourable materials for the most common sensor applications such as typical dielectric characteristics, multilayer capacitors, pyroelectric detectors, piezoelectric transducers, optical sensors [1].The BZT nano composite materials are effectively used in mechano-electric applications such as transducers, sensors and motors for excellent ferroelectric and conductive properties[1]. Hydrothermal technique is one of the reliable methods of synthesizing nano composites [2-3]. In the past 20 years, remarkable efforts have been employed in many perovskite materials such as $BaTiO_3$, PZT, Strontium titanium oxide ($SrTiO_3$) and zinc manganese titanate etc. for useful dielectric applications [4-5]. However, developing pure forms of BZT or PZT using bulk materials, at high temperatures, and exorbitant processing costs remains a difficulty issue [6]. Apart from better density and stiffness of BZT, it's fragile in nature fabrication of fissure-free devices and limiting them to utilize them in electrical applications. To circumvent these limitations, BZT is now combined with PVDF polymer to generate composites with improved dielectric and mechanical performances [7].

The PVDF is a thermoplastic polymer that is highly non-reactive, which is basically produced by the process of polymerization of difluoride. PVDF contains four significant crystallographic, namely (α), (β), (γ) and (δ) phases which are identified by chain confirmation[8-9].The PVDF polymer has several good properties such as self-alignment of charges (Auto poling) ,biocompatible, mechanical flexibility, high breakdown strength, high resistance towards explosive chemicals, cost effectiveness [9-11]. Among all four crystalline phases, it is observed that β phase is having spontaneous polarization capability and conductive sensitivity, due to this characterization which it exhibits electro active phase in PVDF polymers, where in this property can be utilized to develop any dielectric applications. Hydrothermal method is one of the most advantageous techniques which include the fabrication procedure wherein the crystallizing substances vary from high temperature up to 200˚C in the form of liquid at high vapour pressures. It is the synthesis method of single crystal form that depends on the solubility contents of minerals in hot water under high pressure. Here in this hydrothermal process, the device autoclave, which is made of a steel pressure vessel which makes the container airtight and which receives a nutrient and water is poured, which is employed to develop crystals growth [12]. The temperature at gradient is perpetuated at the opposite ends growth of crystals, chamber wherein the solution at higher temperature, the nutrient is dissolved and the cooler end causes seeds to develop growth of the ceramic crystals. As this method has foremost benefits such as they are three-dimensional substrate, automatic self-polarization alignment process, hence hydrothermal autoclave method is selected for polymerization of composites [3] [9]. The polymer nanocomposite is thoughtfully characterized using XRD, SEM, EDX spectroscopy, FTIR, DMA, and DSC thermogram equipments. For the purpose of determining the melting point of PVDF polymer films, In the PVDF polymer films, the influence of the BZT nano composite and its shape, microcrystalline size, and dielectric characteristics were investigated.

The Seybold Report
ISSN 1533-9211
DOI 10.5281/zenodo.7220825

2. EXPERIMENTAL SECTION

2.1 Synthesis of BZT nano composites.

The study's reagents were of high quality and did not require any additional purification before usage. In all of the trials, distilled water was utilized. The Barium nitrate $BaCl_2$ zirconium ox chloride octahydrate ($ZrOCl2•8H_2O$), and titanium isopropoxide ($Ti[OCH(CH_3)_2]4$ were procured from Sigma Aldrich Pvt. Ltd company, which is as per standards. In a typical stoichiometric molar ratio of $BaCl_2$. The equation ratio of $2H_2O$+ $ZrCl_2.8H_2O$+$Ti(C_4H_9O)_4$+2 KOH(0.265:0.181) was mixed in 100 Ml of ethanol was added in drop wise in barium and zirconium aqueous solution followed with continuous stirring. After waiting for 30 minutes, 0.1 M NaOH solution was gradually added to the previously mentioned solution until the BZT co-precipitate was established. A similar co-precipitated gel preparation approach was used in our earlier study to manufacture orthorhombic and other oxides [13-14]. Later the co-precipitated gel is heated through the hot water bath device for about 8 to 9 hours and later dried white powder is crushed and again deposited back in 60ml, deionized water and transferred into 100 ml Teflon beaker and content is hydrothermally treated for 24 hours duration at 180˚C to 200˚C. After processing of treatment, the white residue was collected in the container, where washing process is carried out several times with ethanol and water separately before drying it in the vacuum oven device which is performed at the temperature of 60˚C to 70˚C for the duration of 8 hours.

2.2 Polymerization of BZT-PVDF nanocomposites.

The process for creating BZT-PVDF nanocomposites involved the intercalation of different mixtures of nanoparticles of BZT, weighing 0, 0.5, 1, and 2% weight. The PVDF solution was created by combining 4 grams of PVDF with 100 millilitres of N, N-dimethyl acetamide and allowing it to remain at a temperature of 80˚C for 60 minutes [14]. After adding the necessary quantity of BZT-calcinated nanoparticles to the PVDF solution, it was ultrasonically processed for 60 minutes to achieve the desired dispersion. The cleaned and dust-free glass mould is then filled with the prepared homogenous solution. The BZT-PVDF nanocomposites are now formed by permitting the solution to evaporate. The hybrid nanocomposites thickness range from 0.103mm to 0.183mm.

2.3 Fabrication of pure BZT nano composite pallets.

The BZT composite sample powder was weighed of 0.1gram, sample was grinded by using pestle and mortar, later the grained mortar is transferred to pallet container. The experimental setup was tightly assembled; the pressure about 15Kg/cm^2 is applied manually to the pallet equipment by mechanical hydraulic pressure system. The pallet equipment is maintained with the same pressure for about 2 minutes. Finally the pressure is gradually released and circular disc shaped pallets with dimension of about 1cm diameter and 0.5cm thickness was collected as shown in the Figure 1. The pallets of pure BZT are prepared to study the morphological characteristics of the sample and its electrical properties.

ISSN 1533-9211

DOI 10.5281/zenodo.7220825

Fig1: Circular pure BZT pallet

2.3.1 Fabrication of BZT-PVDF electrode

The as-prepared BZT-PVDF was carefully sliced to the dimensions of 7cmx3cm, and the silver gel was evenly coated using the doctor blade technique in order to manufacture the electrodes to polymer films. The electric wires (leads) are soldered for conductivity for external connections, where it functions as positive and negative terminals, and a little strip of copper-colored conductive tape is manufactured to adhere over the composite materials. The nanocomposite film was coated with silver electrodes on both sides using the same process, and then allowed to dry for 60 to 70 minutes. Figure 2 depicts the fabrication of BZT-PVDF silver electrodes with various BZT concentrations of percentages.

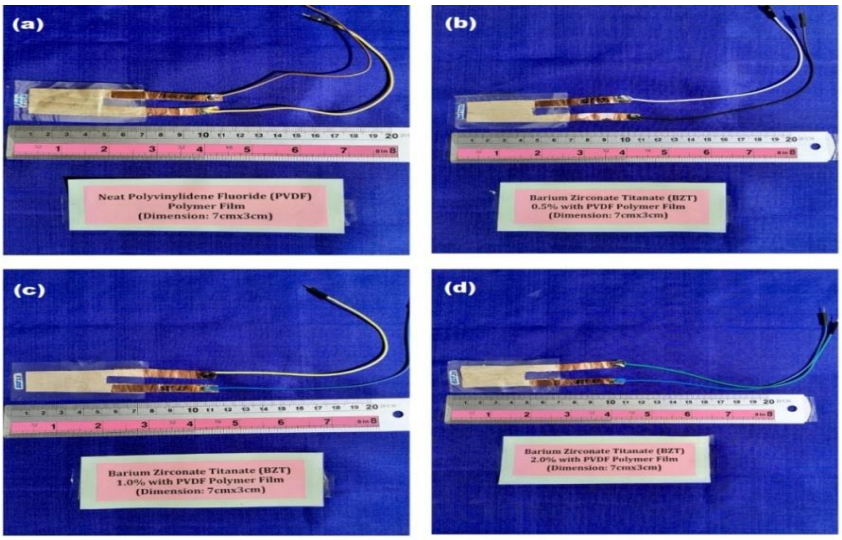

Fig 2: Actual view of (a) Neat PVDF polymer film, (b) 0.5% BZT-PVDF film Polymer, (c) 1.0% BZT-PVDF Polymer film and (d) 2%BZT-PVDF polymer film

2.4 Characterization.

The BZT and PVDF polymer nanocomposites were subjected to X-ray diffraction at room temperature. The materials were examined using a Japanese instrument made by RIGAKU called the Miniflex II Series, which used CuK radiation with a graphite monochromator at a

ISSN 1533-9211

DOI 10.5281/zenodo.7220825

wavelength of around 1.5406 Å.30 kV and 15 mA were the operating voltage and current, respectively. The shape and structure (Composition) of freshly made polymer composites were analyzed using an EDX and SEM Carl Zeiss, 03-81 (Germany). In order to evaluate the hydroxyl radicals, model spectrum 2 series was utilized, 4 cm^{-1} of the resolution, samples were analyzed using FTIR, which was chronicled on the Perkin Elmer (USA) spectrum edition. The current study employed the renowned 3522/3532 LCR Hi Tester impedance analyzer with a ± 0.08% data accuracy to investigate impedance spectra. TA Instruments DMA Q800 analyzer was employed to conduct the DMA. The heating temperatures ranges between -150°C and 400°C were at rates ranging from 0.1°C/min to 20°C/min of heating. The range of 0.01 Hz to 200Hz of the frequency and amplitude range of ± 0.5µm to 10,000 µm.

3. RESULTS AND DISCUSSION

3.1 The phase structure and morphological studies.

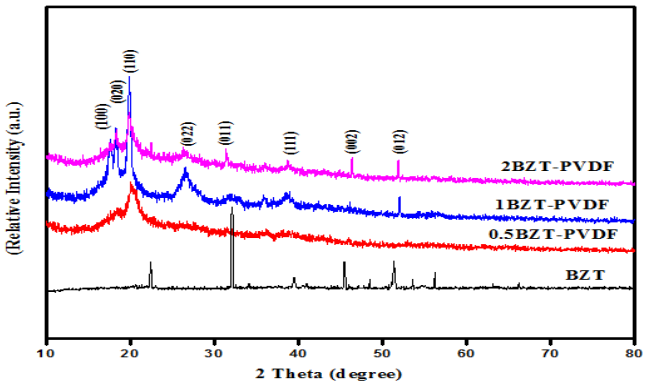

Fig 3: XRD pattern of as prepared BZT with percentage of weight ratio of BZT-PVDF nanocomposite materials

In the current research work, many experiments have done for the synthesis of BZT (Ba ($Zr_{0.25}Ti_{0.75}$) O_3) with the variation in the temperature and time for processing. Among all, the well-matched experimental results of the XRD are compared with the reference data of JCPDS card no: 36-0019 which indicates that BZT nanomaterials homogeneous in composition. The crystalline structures and phase purity were studied by the XRD. The respective powder XRD diffraction peaks of BZT are shown in the figure 3. From the XRD pattern, it represents the 2θ between 0º to 80º, the BZT pattern indicates that the synthesized compound which possesses highly crystalline phase without major impurities.

In the later stages, BZT phase which is synthesized and confirmed, and it is compared with the different ratio weight % namely 0.5% of BZT with PVDF, 1% of BZT with PVDF and 2% of BZT with PVDF which is shown in the figure-3. It has the diffraction pattern range of 2θ between 10 º to 80º where the effective peaks of diffraction at 2θ values of 17.57º, 18.37º, 19.83º, 26.63º, 31.43º, 38.76º, 46.37º and 51.82º is indexed by (100), (020), (110), (002), (011), (111), (002) and (012), which has the reflection Planes of BZT with cubic crystals with space group a = 4.036 Å which correlates to the database of JCPDS card no:36-0019. The diffraction

ISSN 1533-9211

DOI 10.5281/zenodo.7220825

pattern of BZT-PVDF composite film depicts the pseudo-cubic structure and PVDF based α diffraction peak at 2θ = 18.3º for (020) and β diffraction peak is a broad 2θ = 19.8º for (110) respectively, it is associated with BZT-PVDF composite.

3.2 Morphology and elementary study of pure BZT and BZT-PVDF using SEM/EDS.

The SEM analysis was performed to investigate the morphemes of the BZT-PVDF developed nanocomposite, BZT nanocomposite which is pure form synthesized exhibited non-uniform grain as shown in the Figure 4(a). The experimentation was executed using the SEM instrument, HITACHI, S-4200 Vijnana bhavana, Mysore University, Mysore, Karnataka, India. The micrograph depicts the 0.5-1.0 µm size of cluster of crystals are observed in BZT materials which is further dried at temperature about 60ºC. This may also results due to complete diffusion of Zr^{4+} ions in to Ti^{4+} side at optimum temperature and makes more compost of scale down of the material.

Also it is studied that the average grain size is increased (magnified) in BZT sample, sintered at higher temperature. Higher densification plays the vital role in increasing the both electric parameters and physical properties of the specimen in the research study. The energy dispersive spectra EDS of BZT composite material are illustrated in Figure 4(b). The table inside EDS Spectra, shows that elemental composition ceramic sintered at respective range of the temperature. The elements present in the table depicts that BZT material has stoichiometric amount. The final composition of the material is varied as the temperature variation observed weight (%) of the respective element. The Figure 4 depicts that there is no any impurity peak detected in the EDS spectra of the specimen at temperature suggest, formation of pure $BaZr_{0.2}Ti_{0.8}O_3$.

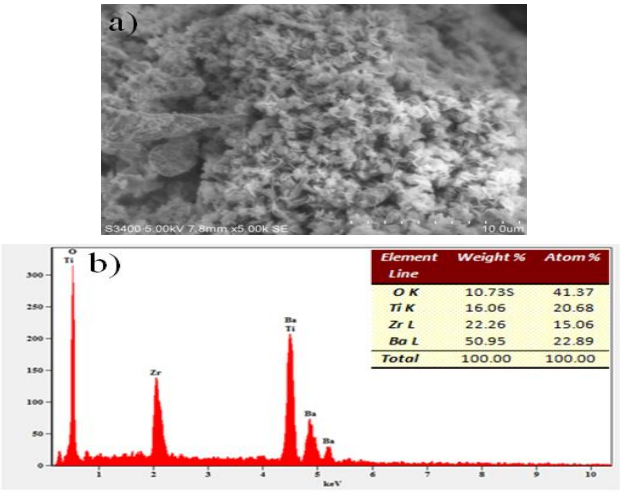

Fig. 4 (a) The SEM images of BZT materials and b) EDS of BZT with inserted table of weight and atom %

DSC analysis is carried out to know the highest range of Crystallinity in the PVDF. The polymer film sample is resistant to tearing in the 27 to 200°C temperature range and

ISSN 1533-9211

DOI 10.5281/zenodo.7220825

endothermic peak (a sharp melting point) at around 167˚C which could be attributing to different crystalline size in the sample. In the DSC thermogram, the peak at low temperature is expected to develop α-form crystalline structure at the same time the peak at high temperature is assigned to the β-form [15]. The results, clearly shows that there is corporeality of both α and β phases in PVDF. The amount of crystallinity was resolved using the equation.

$$\Delta X_c = \frac{\Delta H}{\Delta H_c} \qquad \text{Eq-1}$$

Where, ΔH is the enthalpy liquefying of the composites, ΔHc is the enthalpy liquefying at crystalline PVDF polymer. The ΔHc for pure PVDF is about 104.7 J/g [15].

3.3 FTIR Spectroscopy Analysis.

To investigate the bonding of a chemical and structure of molecules of the as-prepared nanocomposites, Fourier infrared (FT-IR) spectroscopy was performed, and the outcome is shown in the Fig 5. The FT-IR spectrums of pure BZT and PVDF are consistent, it was insured the correct identification of phases. The Fig-5 depicts the absorbance spectra of BZT based PVDF films at different weight percentage ratio. The band at 550cm^{-1} corresponds to the Ti-O bond; vibration of the BZT synthesized material [16]. The FTIR figure shows the absorption of typical IR bands of ethanol which is varied in the range of 2800-3000cm^{-1} and 3000-3400cm^{-1} and these bands are attributed to be C-H stretching and O-H vibration stretching respectively [17].The range of 400-600cm^{-1} is the absorption band is often assigned to the formation of Zr-O and Ti-O stretching vibration [18]. The peaks at 578cm^{-1} and 525cm^{-1} can be assigned to the vibrations of TiO_6 and ZrO_6 octahedral. The results of FTIR spectra are compatible with XRD analysis for confirming that formation temperature of BZT materials at temperature of 180˚C.

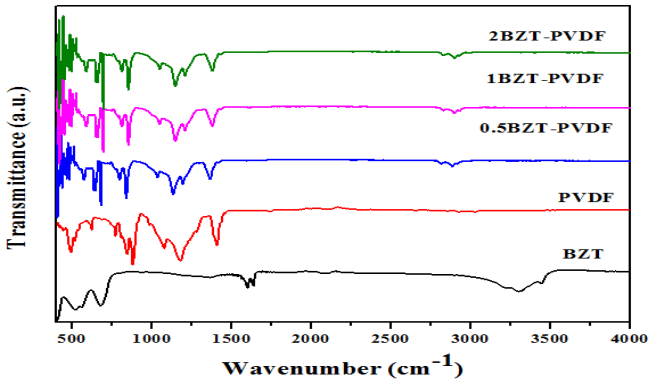

Fig 5: FTIR spectrums of pure BZT and BZT-PVDF composite films

The infrared spectrum of BZT-based PVDF intensification from 10 to 50% of nano composites as shown in the FTIR Fig-5. The presence of PVDF's-phase is authenticated by the assimilation bands values ranges at 511 and 840 cm^{-1}in infrared spectra [19]. The BZT nanocomposite strongly absorbs at 700cm^{-1}[19], rendering it difficult for composites with ceramic compositions beyond 20% weight to detect the band of 511cm^{-1}. This implies that as BZT levels rise, BZT peaks predominate, weakening the prominence of PVDF peaks. The corresponding vibration bands at the range of values of 764,795cm^{-1}related to PVDF films,

The Seybold Report
ISSN 1533-9211
DOI 10.5281/zenodo.7220825

778cm^{-1},795cm^{-1}, 834cm^{-1}, and 840cm^{-1} have been attributed to the γ phase and β phase, respectively [20–36]. Remarkably, after introducing BZT into PVDF polymer, the FT-IR signal changes in small ratio, with minor decrease in the intensity with that of pure PVDF without much modification in their position.

3.4 Dynamic Mechanical Analysis of plain PVDF polymer film

Dynamic mechanical analysis (DMA) is an intuitive approach for analyzing the dynamic modulus and damping coefficient, this is during the changes of crystalline structure. It used as a fundamental tool to determine the viscoelastic properties and flow behaviour of the materials. It is very fragile method which defines dynamic mechanical properties of polymeric composites and polymers. The procedure of the experiment as follows, initially the machine is set to multi- frequency mode, a PVDF polymer film of the dimensions of 10 mm in width, 11.140 mm in length, and 0.06mm in thickness, with a rectangular shape is cut mounted into the sample holder. Testing is first commenced with the room temperature of 28˚C. After the specimen is fixed in the holder, lid is closed up setting up the temperature of 6˚C in the system. The experiment is preceded until the sample deforms and respective temperature is noted down. Now the result graph shows the important mechanical behaviour such as storage modulus (MPa), Loss tangent and tan delta. The DMA experimentation continuous till PVDF film deforms and shows the final reading. [37]. The PVDF is also used as a vibration damping system, medical, ultrasound and microphones, pressure sensors, acoustic sensor, shock sensor, hydrophones, strain measurement sensor and low cost accelerometer applications [38]. The most popular operational modes for DMA are temperature and frequency sweeps, which offer complex (E*), storage (E′), and loss moduli (E″). In DMA test, the energy contained in the specimen is shown by the storage modulus (E′), whereas the energy lost is shown by the loss modulus (E″). Glass transition temperature (Tg) is computed using the expression tan (δ) = E″/ E′, which is known as the internal friction ratio (internal friction) as shown in the Fig 6.

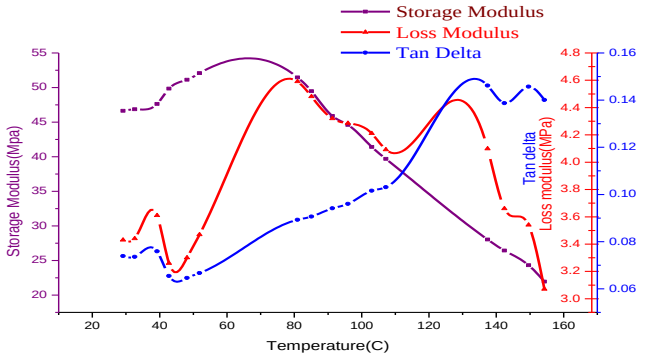

Fig 6: E′, E″, tanδ vs Temperature

Storage modulus determined from the sample reflects the elastic behaviour and flow of a material when deformed. The response of a viscous behaviour of the material gives the Loss modulus and the energy lost which is known as damping [39]. Storage modulus is influenced by its elastic behaviour and loss modulus is influenced by its viscous behaviour. In viscoelastic

The Seybold Report
ISSN 1533-9211
DOI 10.5281/zenodo.7220825

liquid, viscous behaviour is higher than elastic behaviour. In the present work from Fig.6, storage modulus (E′) is greater than the loss modulus (E″) and is known as viscoelastic solid. In the viscoelastic solid, the elastic behaviour is higher than the viscous property, wherein this characteristic allows managing higher stress and deformation, which is essential for the application of pressure sensor. In this type of material, after the removal of external pressure the material regains the origin its shape [40]. The response of the PVDF material which has been observed in the above graph, this behaviour is reported from the curve of tanδ which has a peak that was identified as the glass transition temperature, which is around -40°C. This is connected to a significant reduction in the storage modulus in that region, and also previous studies have resulted that additional tan peak at temperatures higher than Tg [41-45] which has come strong evidence. Hence we can conclude that Viscoelastic solid material that was selected i.e. Storage modulus > loss modulus. T_g by Storage modulus Peak = 67.7 °C, T_g by Loss modulus Peak = 78.82 °C, T_g by tanδ Peak = 133.51 °C.As the E' >E″ hence the PVDF film will be a gel-like structure [46].

4. DIELECTRIC STUDIES OF BZT BASED PVDF POLYMER FILMS WITH DIFFERENT WEIGHT PERCENTAGE (0.5, 1 & 2%)

The electrical properties of PVDF polymer along with BZT-PVDF nanocomposites at different frequencies are calculated and the outcome is represented in the Fig.7, the dielectric constant is evaluated using the below formula.

$$\varepsilon = \frac{C_p d}{\varepsilon_o A} \qquad \text{Eq-2}$$

Where, Capacitance in Farads is denoted by Cp, the film's thickness ‘d’ is measured in meters, free space has a permittivity of ε_0 (8.854×10^{-12} F/m) and ‘A’ represents area of cross section in m^2. The PVDF Dielectric conductivity is compared it with BZT nanocomposite having weight % (0.5, 1 & 2%) with respect to the frequency is plotted in the Fig 7.

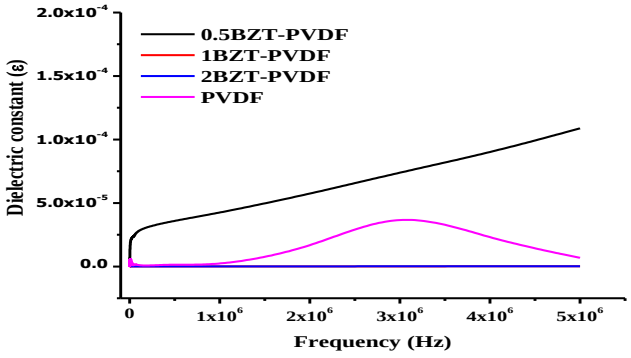

Fig 7: Dielectric constant of PVDF nanocomposites with different concentrations of BZT nanoparticles

It was noticed that the dielectric constant at 1.0×10^{-4} for frequency 5×10^6 Hz is compared with the pure PVDF film, 1 BZT-PVDF and 2 BZT-PVDF films. The PVDF phase acts as insulating

ISSN 1533-9211

DOI 10.5281/zenodo.7220825

phase conforming to 0.5 wt% as an optimum ratio. On the other side, the lesser the dielectric characteristics results from lager BZT component. The variations of dielectric properties in this work were compatible and observed the similar for PZT/P(VDF-TrFE)[47],$BaTiO_3$/PVDF and $(Bi_{0.5}Na_{0.5})_{0.94}Ba_{0.06}TiO_3$/P(VDF-TrFE)[48-49]materials. The notable quantity of BZT in the PVDF matrix may the cause of drop in dielectric constant which can be depicted at rising concentrations of BZT above 0.5 wt %. Firmino Mendes et al. [50]. The PZT percentage concentration in PVDF on dielectric properties had been investigated. Also reported that, percentage of BZT and its grain size structure values increase that are primarily proportionate to the BZT material and independent of PVDF phase.

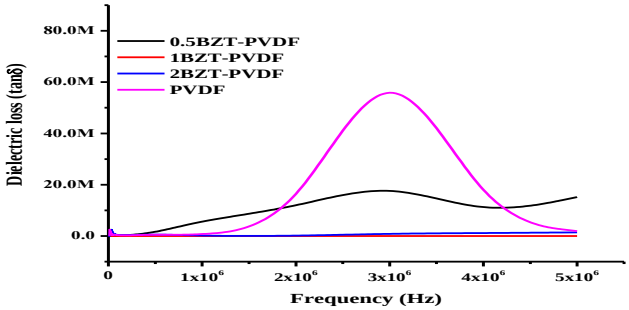

Fig 8: Dielectric loss (tan δ) of PVDF nanocomposite with different concentrations of BZT nanoparticles

The above Fig.8 depicts the variation in dielectric loss (tan δ) with frequency of BZT-based PVDF nano composites. The pure PVDF with increasing of the dielectric loss at the frequency of about $1x10^6$ and reached maximum dielectric loss altitude at the frequency at $3x10^6$ Hz and declines dramatically and remains nearly constant of dielectric loss at the frequency of about $5x10^6$ Hz. The 0.5 BZT-PVDF is gradually increasing the conductivity loss while the frequency increases and it demonstrates maximum dielectric loss about 20.0M at the frequency of $3x10^6$ and further gradually declines the conductivity loss of about 10.0M at frequency of $4x10^6$ Hz and proceeding, the dielectric loss increases up to 20.0M at the frequency of $5x10^6$ Hz [51,52]. The conductivity of 1% BZT-PVDF composite film remains constant even at higher frequencies. Conductivity has somewhat improved of 2%BZT-PVDF slightly when the frequency is increased, when it is compared with 1%BZT-PVDF film. Here in this work, PVDF showed maximum dielectric loss with respect to frequency and gradually decreases when it is compared with 0.5, 1 & 2% wt of BZT based PVDF polymer. From the graph of Fig.8, it shows that 0.5%BZT-PVDF is exhibition maximum dielectric loss with respect to frequency, and further increase of BZT to 1% and 2 wt%, dielectric loss is reduced. It is hypothesized that the surge in loss at high frequencies is triggered by the PVDF process and glass transition relaxation [29].

ISSN 1533-9211

DOI 10.5281/zenodo.7220825

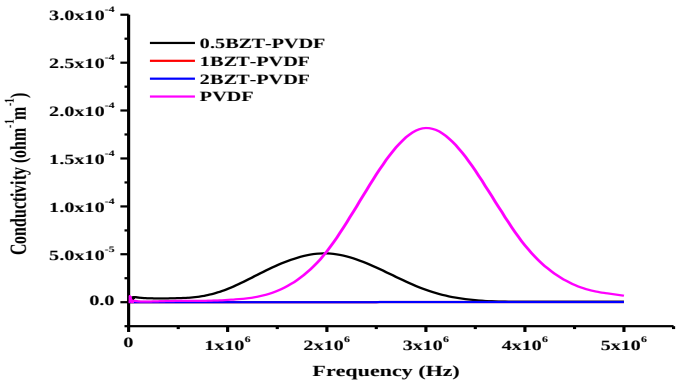

Fig 9: Dielectrical conductivity of PVDF nanocomposites with different concentrations of BZT nanoparticles

The above Fig.9 shows how conductivity is frequency-dependent of the pure PVDF, 0.5 BZT-PVDF, 1BZT-PVDF and 2BZT-PVDF based polymers at room temperatures. The a.c conductivity of the as-prepared nanocomposites is calculated by using the equation given below.

$$\sigma_{ac} = \frac{(G)X(t)}{(A)} \qquad \text{Eq-3}$$

The thickness is represented by 't' (0.47 mm), 'A' represents the area of polymer (2.0096 cm^2), and 'G 'is the conductivity. The conductivity upsurge with the accession in frequency and continues approximately constant at high frequency. The neat PVDF polymer depicts maximum conductivity of about $1.7x10^{-4}$with respect to the frequency of about 3 x 10^6 Hz and conductivity declines and come to stable at the value of $5x10^6$ Hz. The different weight percentage of composites materials 0.5 BZT-PVDF, 1 BZT-PVDF and 2 BZT-PVDF based polymers, among these only 0.5BZT-PVDF exhibits the maximum conductivity with respect to the frequency, from the Fig.9, the graph shows that, the conductivity auguments with respect to the frequency of $1x10^6$ Hz, has attained highest frequency at $2x10^6$ and it gradually decline to remain constant at the frequency of 3.5 x 10^6 Hz. Both 1 BZT-PVDF and 2 BZT-PVDF based polymer films are not increasing any dielectric conductivity and it is maintained constant even at high frequency. Moreover, their conductivity was enhanced with previous work studies, which demonstrates that they were good insulator [51, 53].

The electrical modulus M* is used to study the electrical relief processes which coincides to the relief of the field of electricity in the nanocomposites polymer when the electric movement remains consistent and is detained as a combining the materials of complex permittivity which could be obtained from the following equations.

$$M^* = \frac{1}{\varepsilon^*} = M_1 + jM_2 \qquad \text{Eq-4}$$

The Seybold Report
ISSN 1533-9211
DOI 10.5281/zenodo.7220825

The below equation 5 and 6, represents real and imaginary modulus.

$$M' = \frac{\varepsilon_1}{\varepsilon_1^2+\varepsilon_2^2} \qquad \text{Eq-5}$$

$$M'' = \frac{\varepsilon_1}{\varepsilon_2^2+\varepsilon_2^2} \qquad \text{Eq-6}$$

The dielectric loss was calculated using the below equation;

$$\epsilon'' = \tan\delta \qquad \text{Eq-7}$$

The real modulus (M') and imaginary modulus (M'') of electric modulus (M^*) is dependent on electrical frequency, with different BZT combinations are as shown in the figure-10.

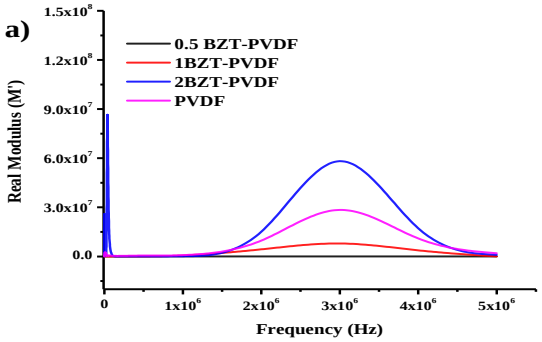

Fig 10: (a) Real modulus Imaginary modulus of PVDF concerning the different frequencies

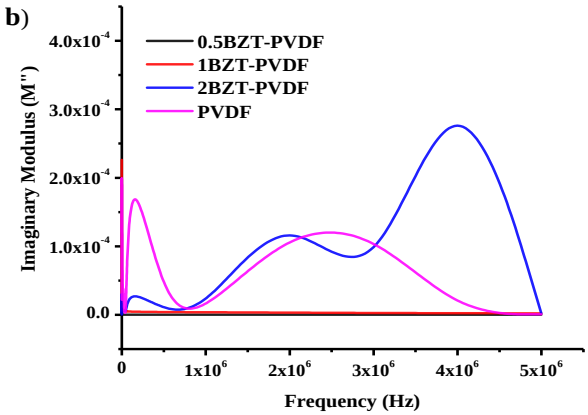

Fig 10: (b) Imaginary modulus of PVDF concerning at different frequencies and concentrations of BZT nanocomposites.

When compared to pure PVDF, Figure 10(a) shows the frequency that is controlled and dependent change of the real component of electrical modulus (M') at various weight

The Seybold Report
ISSN 1533-9211
DOI 10.5281/zenodo.7220825

percentages of BZT materials. The graph suggests that (M') at $1.5x10^6$ is almost zero at lower frequencies, while it repeatedly rises with increasing frequency and it depicts maximum electrical modulus (M') of all the weight percentage of BZT-PVDF at a frequency at the frequency of $3x10^6$ and gradually decreases to become zero, indicating as the relaxation of the electrical modulus (M') at the frequency of $5x10^6$[54, 55]. Out of all materials, it is found that 2BZT-PVDF which exhibited maximum electrical (M') of $6.0x10^7$ which is followed by the neat PVDF polymer film which shows $3x10^6$ and 1% weight depicts $1x10^6$. In the figure-10(b), frequency-dependent swing of the electrical modulus imaginary part (M") values at different weight percentages of BZT nano composite materials which is compared against the pure PVDF material. It is noted that the peak value of (M" Max) evolves towards higher frequency with varying the weight percentages of BZT based PVDF polymers. At initial zero frequency, pure PVDF exhibits maximum imaginary modulus (M") at $1.5x10^{-4}$ with sharp curve and gradually deteriorates to become zero frequency at $1x10^6$ is depicted in the Fig.10 (b). Moving further it show maximum imaginary modulus (M") about 1.0×10^{-4} with exhibits the frequency in dull along with maximum at $2.5x10^6$ and declines to become zero at 4.5×10^6 frequency. At zero frequencies, imaginary modulus graph (M") of 2 % BZT-PVDF polymer eventually increases and shows maximum of $3.0x10^{-4}$ imaginary modulus (M") at $4x10^6$ frequency and suddenly declines to become zero imaginary modulus at $5x10^6$.

5. CONCLUSION

The hydrothermal methodology was employed after the sol-gel technique to synthesize BZT nanoparticles featuring agglomerated crystals that spanned in size from 0.5 to 1.0 µm. The BZT nano materials are synthesized, and the solvent casting process is used to polymerize them along with the PVDF matrix. As the inference, the hydrothermal method has the significant advantages for self-alignment or polling, the fabrication of lead-free conductive polymer materials and also results in ultrahigh quality PVDF blended with nano composites polymer films. In the current work, the phase of purity and existence of BZT nano particle blended into the PVDF polymer matrix, which were confirmed by XRD, and SEM and it reveals that BZT has well dispersed in the PVDF material. The PVDF polymer exhibited satisfactory dynamic mechanical properties for use research studies. The filler material influences the crystallization of morphology of the β-PVDF phase, the effective dielectric characteristics of BZT-PVDF were investigated and further the outcome reveals that the weight percentage of BZT in the PVDF nanocomposite shows a pivotal role in enhancing the dielectric properties.

In our study it reveals that the value of 0.5%BZT-PVDF has highest dielectric studies of Dielectric loss, conductivity, constant when compared to other weight percentage composition of PVDF polymers such as 1%BZT-PVDF and 2%BZT-PVDF. Wherein it could be observed that increase in BZT loading tend to decline in the extent of β phase and frequently reduced dielectric coefficient. From the dielectric studies it also clearly shows that plain PVDF polymer exhibits highest peaks. The change of non-polar α PVDF part to polar β PVDF phase is also attributable to the redistribution of electric charge in the nano composite. Due to the phase's configuration in the PVDF, it is clear that it is good sign for the application of materials in pressure sensor application.

The Seybold Report
ISSN 1533-9211
DOI 10.5281/zenodo.7220825

Author Contributions Statement

Authors 1, 2, 3 wrote the main manuscript and 4, 5 prepared the figures 1-10. All authors reviewed the manuscript.

Data availability statements

Data sharing not applicable to this article as no datasets were generated or analyzed during the current study.

Acknowledgements

The authors would like to acknowledge the University of Mysore, Manasagongotri, Mysore and Visvesvaraya Technological University (VTU) Belgavi, Karnataka. Authors would like to extend thanks to the University of Mangalore for SEM and EDX analysis. Mr. Rakesh. M would like to express his gratitude to family members and friends for encouraging him with their love and support.

Declaration of the Competing Interest

The authors declare that no known competing financial delights or personal association with the editorial board members that could have appeared to influence the work reported in this paper.

Funding

"During the preparation of this work, the authors state that they did not receive any funding, grants, or other support of any kind".

References

1) Chen, X.G, Two-Dimensional Layered Perovskite Ferroelectric with Giant Piezoelectric Voltage Coefficient. Journal of the American Chemical Society, 142(2), 2020, p. 1077-1082.

2) Elena Aksel and Jacob L. Jones; Free Piezoelectric Materials for Sensors and Actuators, SensorsDept, University of floridaAdvances in Lead March 2010., IISN 1424-8220,March 2010, 1-9.

3) Yuan Deng Liliu, Hydrothermal synthesis and characterization of nanocrystalline PZT powders;Elsevier ,Volume 57, Issue 11, March 2003, 20-27.

4) Wu, L.K, Recent advances in the preparation of PVDF-based piezoelectric materials, Nanotechnology Reviews,11(1): 2022, p. 1386-1407.

5) Rached, A, Structural, optical and electrical properties of barium titanate, Materials Chemistry and Physics,267: p. 124600,2021, 1-6.

6) Nguyen, M.D, Effect of dopants on ferroelectric and piezoelectric properties of lead zirconate titanate thin films on Si substrates. Ceramics international, 40(1), 2014, p. 1013-1018.

7) Piezo film sensors technical manual. Images SI Inc. Sensors product division State Island NY 252, 2016, 82-87.

8) BinoyBera,Madhumita das Sarkhar, Piezoelectricity in PVDF and Piezoelectric based a Nanogenerator: A concept,IOSR Journal of Applied Physics,e-ISSN:2274-4861, Volume9, Issue 3,June 2017, 1-5.

9) Shuaibing Guo,Xuexin Duan,MengyingXie,Kean Chin Aw and QiannanXue, Composites, Fabrication and Application of Polyvinylidene Fluoride for Flexible Electromechanical Devices: A Review,Micromachines,MPDI, 3 December 2020, 52-57.

10) N. Murayama,K.Nakamura,H.Obara, M.Segawa, The strong piezoelectricity in polyvinylidene fluroide (PVDF), Elsevier, Volume14, Issue 1, 2002, 1-8.

11) Sukitpaneenit, P. and T.-S. Chung, Molecular elucidation of morphology and mechanical properties of PVDF hollow fiber membranes from aspects of phase inversion, crystallization, and rheology, in Hollow Fiber Membranes, Elsevier, 2021 p. 333-360.

The Seybold Report
ISSN 1533-9211
DOI 10.5281/zenodo.7220825

12) Takeshi Morita, Piezoelectric Materials Synthesized by the Hydrothermal Method and Their Applications, Materials, 9 December 2010, 20-25.

13) Girish, H, Hydrothermal synthesis and characterization of polycrystalline gadolinium aluminum perovskite (GdAlO3, GAP). Mater Sci-Poland, 2015. 33: p. 301-305.

14) E. Yilmaz and M. Soylak, 15-Functionalized nanomaterials for sample preparation methods, in Handbook of Nanomaterials in Analytical Chemistry, Elsevier, 2020, pp. 375-413.

15) T. Greeshma, R. Balaji, S. Jayakumar, PVDF Phase Formation and Its Influence on Electrical and Structural Properties of PZT-PVDF Composites, Ferroelectr. Lett. Sect. 40,2013, 41-55.

16) S. Liu, S. Xue, S. Xiu, B. Shen, and J. Zhai,Surface-modified Ba (Zr0. 3Ti0. 7) O3 nanofibers by polyvinylpyrrolidone filler for poly (vinylidene fluoride) composites with enhanced dielectric constant and energy storage density,Scientific reports, vol. 6, pp. 1-11, 2016.

17) J. Coates, Interpretation of infrared spectra, a practical approach, 2000, 1-8.

18) P. Seeharaj, B. Boonchom, P. Charoonsuk, P. Kim-Lohsoontorn, and N. Vittayakorn, Barium zirconate titanate nanoparticles synthesized by the sonochemical method, Ceramics International, vol. 39, 2013, pp. S559-S562.

19) R. Gregorio, M. Cestari, and F. Bernardino, Dielectric behaviour of thin films of β-PVDF/PZT and β-PVDF/BaTiO3 composites, Journal of Materials Science, vol. 31, 1996, pp. 2925-2930,.

20) J. Curie and P. Curie,Développement par compression de l'électricité polaire dans les cristaux hémièdres à faces inclinées, Bulletin de minéralogie, vol. 3, 2015, pp. 90-93.

21) J. J. Stroyan, Processing and characterization of PVDF, PVDF-TrFE, and PVDF-TrFE-PZT composites,Washington State University, 2004, 36-45.

22) C. Williams and R. B. Yates,Analysis of a micro-electric generator for microsystems,Sensors and actuators A: Physical, vol. 52, 1996, pp. 8-11,.

23) Y. Bormashenko, R. Pogreb, O. Stanevsky, and E. Bormashenko,Vibrational spectrum of PVDF and its interpretation,Polymer testing, vol. 23, 2004, pp. 791-796,.

24) T. Boccaccio, A. Bottino, G. Capannelli, and P. Piaggio,Characterization of PVDF membranes by vibrational spectroscopy, Journal of membrane science, vol. 210, 2002, pp. 315-329.

25) J. Li, C. Wang, W. Zhong, P. Zhang, Q. Wang, and J. Webb,Vibrational mode analysis of β-phase poly (vinylidene fluorid, Applied physics letters, vol. 81, 2002, pp. 2223-2225.

26) S. Lanceros-Mendez, J. Mano, A. Costa, and V. H. Schmidt,FTIR and DSC studies of mechanically deformed β-PVDF films, Journal of Macromolecular Science, Part B, vol. 40, 2001, pp. 517-527.

27) S. Satapathy, S. Pawar, P. Gupta, and K. Varma,Effect of annealing on phase transition in poly (vinylidene fluoride) films prepared using polar solvent", Bulletin of Materials Science, vol. 34, 2011, pp. 727-733.

28) B. P. Neese, Investigations of structure-property relationships to enhance the multifunctional properties of PVDF-based polymers: The Pennsylvania State University, 2009, 1-7.

29) J. Gregorio, Rinaldo and M. Cestari,Effect of crystallization temperature on the crystalline phase content and morphology of poly (vinylidene fluoride),Journal of Polymer Science Part B: Polymer Physics, vol. 32,1994, pp. 859-870.

30) G. K. Ottman, H. F. Hofmann, A. C. Bhatt, and G. A. Lesieutre,Adaptive piezoelectric energy harvesting circuit for wireless remote power supply, IEEE Transactions on power electronics, vol. 17, 2002, pp. 669-676.

The Seybold Report
ISSN 1533-9211
DOI 10.5281/zenodo.7220825

31) J. L. González, A. Rubio, and F. Moll,Human powered piezoelectric batteries to supply power to wearable electronic devices, International journal of the Society of Materials Engineering for Resources,vol. 10, 2002, pp. 34-40.

32) J. M. Rabaey, M. J. Ammer, J. L. Da Silva, D. Patel, and S. Roundy,PicoRadio supports ad hoc ultra-low power wireless networking, Computer, vol. 33, 2000, pp. 42-48.

33) J. Gragg, The emergence of RFID technology in modern society,Oregon State University, 2003, 1-7.

34) S. Roundy, P. K. Wright, and J. M. Rabaey, Energy scavenging for wireless sensor networks,in Norwell, ed: Springer, 2003, pp. 45-47.

35) A. Khaligh, P. Zeng, and C. Zheng, "Kinetic energy harvesting using piezoelectric and electromagnetic technologies—state of the art," IEEE transactions on industrial electronics, vol. 57, pp. 850-860, 2009.

36) M. Kobayashi, K. Tashiro, and H. Tadokoro, Molecular vibrations of three crystal forms of poly (vinylidene fluoride), Macromolecules, vol. 8, 1975, pp. 158-171.

37) Piezo film sensors technical manual. Images SI Inc. Sensors product division State Island NY 252, 2016, 1-6.

38) Jain A, Prashanth KJ, Jayanth KS, Sharma AK, Typical properties and specific applications of piezoelectric polymer, Int J Mater Sci Eng., 3(4), 2015, 327-45.

39) Anshuman shrivastav, Introduction to plastic engineering- plastic properties and testing, plastic design library, 2018, 71-77.

40) Davoodi B., Muliana A., Tscharnuter D, Analyses of viscoelastic solid polymers undergoing degradation, Mech Time-Depend Mater19, 2015, 397–417

41) Malmonge, Luiz Francisco, Simone do Carmo Langiano, João Manoel Marques Cordeiro, Luiz Henrique Capparelli Mattoso, and José Antonio Malmonge, Thermal and mechanical properties of PVDF/PANI blends, Materials Research 13, 2010, 465-470.

42) Li, Y., Oono, Y., Kadowaki, Y., Inoue, T., Nakayama, K., & Shimizu, H. (2006), A novel thermoplastic elastomer by reaction-induced phase decomposition from a miscible polymer blend, Macromolecules, 39(12), 4195-4201.

43) Liu, Zhehui, Philippe Maréchal, and Robert Jérôme, DMA and DSC investigations of the β transition of poly (vinylidene fluoride), Polymer 38, no. 19, 1997, 4925-4929.

44) A. Linares, J.L. Acosta, Tensile and dynamic mechanical behaviour of polymer blends based on PVDF, European Polymer Journal, Volume 33, Issue 4, 1997, Pages 467-473.

45) Tsagaropoulos, George, and Adi Eisenberg.Dynamic mechanical study of the factors affecting the two glass transition behavior of filled polymers. Similarities and differences with random ionomers, Macromolecules 28.18, 1995, 6067-6077.

46) Kalimuldina G, Turdakyn N, Abay I, Medeubayev A, Nurpeissova A, Adair D, Bakenov Z. A Review of Piezoelectric PVDF Film by Electrospinning and Its Applications, Sensors (Basel), 20(18):5214, 2020 Sep 12, 21-26.

47) M. Dietze and M. Es-Souni, Structural and functional properties of screen-printed PZT–PVDF-TrFE composites, Sensors and Actuators A: Physical, vol. 143, , 2008,pp. 329-334.

48) J. Kułek, I. Szafraniak, B. Hilczer, and M. Połomska, Dielectric and pyroelectric response of PVDF loaded with BaTiO3 obtained by mechanosynthesis,Journal of Non-Crystalline Solids, vol. 353, 2007, pp. 4448-4452,.

The Seybold Report
ISSN 1533-9211
DOI 10.5281/zenodo.7220825

49) X. Wang, K. H. Lam, X. Tang, and H. Chan, Dielectric characteristics and polarization response of lead-free ferroelectric (Bi0. 5Na0. 5) 0.94 Ba0. 06TiO3–P (VDF-TrFE) 0–3 composites," Solid state communications, vol. 130, 2004, pp. 695-699.

50) S. Firmino Mendes, C. M. Costa, V. Sencadas, J. Serrado Nunes, P. Costa, R. Grégório, Effect of the ceramic grain size and concentration on the dynamical mechanical and dielectric behavior of poly (vinilidene fluoride)/Pb (Zr0. 53Ti0. 47) O3 composites,Applied Physics A, vol. 96, 2009, pp. 899-908.

51) Q. Chi, J. Dong, G. Liu, Y. Chen, X. Wang, and Q. Lei, Effect of particle size on the dielectric properties of 0.5 Ba (Zr0. 2Ti0. 8) O3–0.5 (Ba0. 7Ca0. 8) TiO3/polyvinylidene fluoride hybrid films,Ceramics International, vol. 41, 2015, pp. 15116-15121,

52) B. Luo, X. Wang, Y. Wang, and L. Li, Fabrication, characterization, properties and theoretical analysis of ceramic/PVDF composite flexible films with high dielectric constant and low dielectric loss,Journal of Materials Chemistry A, vol. 2, 2014, pp. 510-519.

53) L. Zhang, X. Shan, P. Wu, and Z.-Y. Cheng, Dielectric characteristics of CaCu3Ti4O12/P (VDF-TrFE) nanocomposites,Applied Physics A, vol. 107, 2012, pp. 597-602.

54) K. L. Routray, S. Saha, and D. Behera, DC Electrical Resistivity, Dielectric, and Magnetic Studies of Rare-Earth (Ho3+) Substituted Nano-Sized CoFe2O4,physica status solidi (b), vol. 256, 2019, p. 1800676,.

55) S. B. Aziz, A. S. Marf, E. M. Dannoun, M. A. Brza, and R. M. Abdullah,The study of the degree of crystallinity, electrical equivalent circuit, and dielectric properties of polyvinyl alcohol (PVA)-based biopolymer electrolytes,Polymers, vol. 12, 2020, p. 2184.